

Kivanc Yangi, MD¹; Egemen Gok¹; Arturo Luna Arroyo, MD¹; Michael T. Lawton, MD¹; Mark C. Preul, MD¹

1: The Loyal and Edith Davis Neurosurgical Research Laboratory Department of Neurosurgery, Barrow Neurological Institute, St. Joseph's Hospital and Medical Center, Phoenix, Arizona, United States

Introduction

Anatomical triangles are critical microsurgical landmarks that guide neurosurgeons to deep-seated brainstem and skull-base targets. Despite their potential relevance, the supratrigeminal (STT) and infratrigeminal (ITT) triangles remain insufficiently characterized in the literature. These regions may function as surgical corridors to the anterolateral pons and upper cerebellopontine cistern, providing access to supra- and infratrigeminal safe entry zones (SEZs).

This study aims to define the anatomical and surgical significance of the STT and ITT through detailed descriptive and quantitative analyses, including boundary delineation, expansion potential, and extent of surgical exposure, to optimize their use in microsurgical approaches.

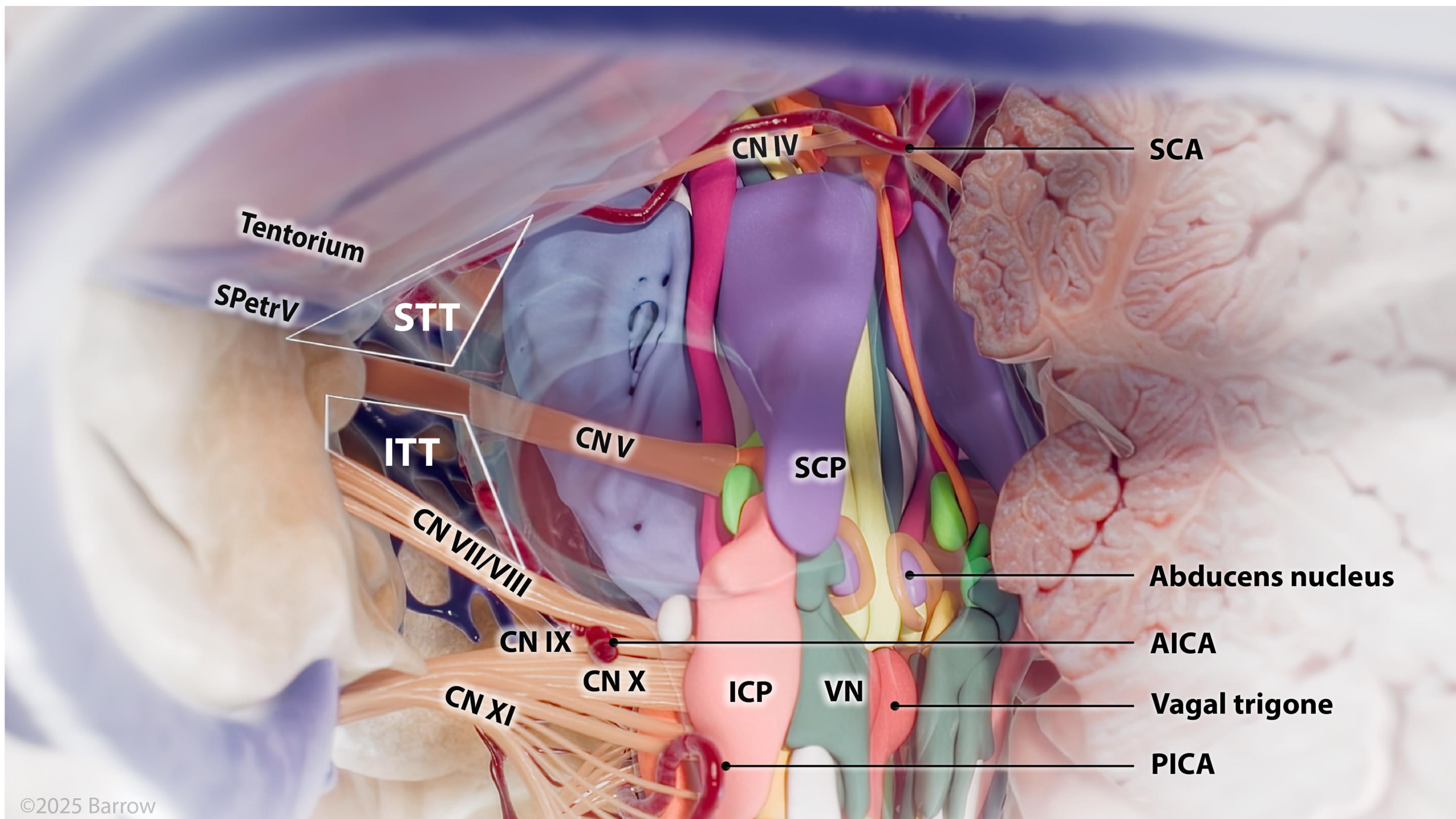


Figure 1: Artist's illustration of the supratrigeminal (STT) and infratrigeminal (ITT) triangles and their surrounding anatomical structures as visualized through the retrosigmoid surgical corridor.

Methods

Eight formalin-fixed, latex-injected cadaveric heads (16 sides) were dissected via an extended retrosigmoid craniotomy using a transcerebellopontine angle approach, with bilateral exploration of the supratrigeminal (STT) and infratrigeminal (ITT) triangles. Neuronavigation-assisted measurements were performed to quantify triangle dimensions under both standard and expanded exposures. Statistical analyses were conducted using R software (v4.4.3). Two additional cadaveric specimens were used to illustrate relevant brainstem anatomy. Ultrahigh-resolution 7-Tesla MRI and 3D modeling were employed to visualize associated white matter tracts.

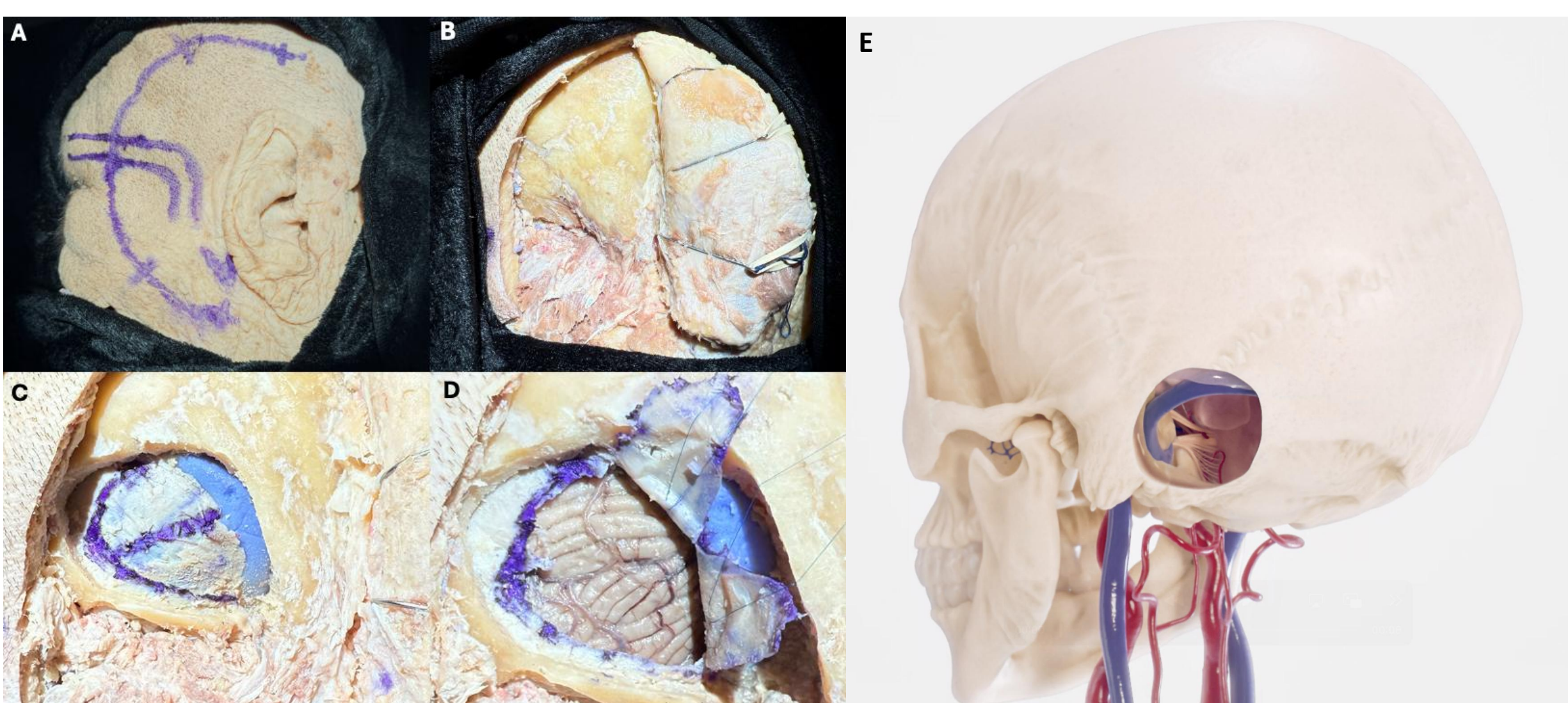


Figure 2: Cadaveric dissections (A–D) demonstrating the skin incision, craniotomy margins, and dural opening. 3D rendering (E) illustrates the bony resection boundaries of the extended retrosigmoid craniotomy.

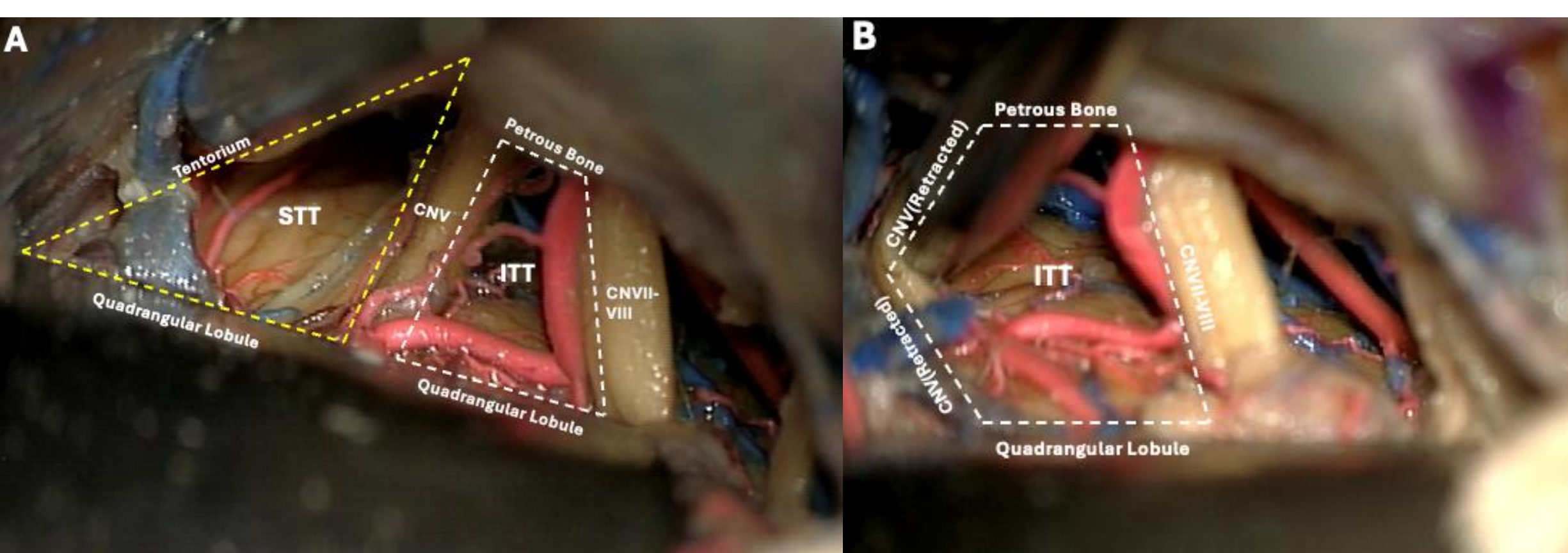


Figure 3: Cadaveric dissections demonstrating the anatomical boundaries of the STT and ITT (A). Panel B highlights the expanded brainstem exposure achieved through the ITT following trigeminal nerve retraction.

Results

The STT is bordered by the QBL posteriorly, tentorium superiorly, and CN V inferiorly. Standard brainstem exposure through the STT averaged $64.6 \pm 27.6 \text{ mm}^2$ and increased significantly with border retraction (all $p < 0.001$), reaching a maximal theoretical exposure of $168.1 \pm 48.9 \text{ mm}^2$ with combined retraction. The ITT is bordered by the QBL posteriorly, CN V superiorly, SVN inferiorly, and petrous bone anteriorly. Baseline exposure measured $73.9 \pm 15.2 \text{ mm}^2$ and expanded significantly with retraction of individual borders (all $p < 0.001$), with a maximal potential exposure of $149.6 \pm 30.9 \text{ mm}^2$. Functionally, the STT provides a favorable trajectory to lesions of the upper cerebellopontine cistern and access to Meckel's cave and adjacent vascular structures, whereas the ITT offers more direct exposure to the porus trigeminus and porus acousticus.

STT Measurements	Explanation	Measurements (Mean \pm SD)
Edge lengths, mm		
Posterior	QBL	11.95 ± 3.73
Superior	Tentorium	18.72 ± 2.83
Inferior	Upper edge of CN V	11.26 ± 2.35
Area of STT, mm²		
STT Vertex Angles, °		
Anterior vertex	Tentorium - CN V	37.01 ± 13.03
Posteroinferior vertex	QBL - CN V	107.39 ± 16.82
Posterosuperior vertex	QBL - Tentorium	35.6 ± 13.96

Table 1: Measurements of STT

ITT Measurements	Explanation	Measurements (Mean \pm SD)
Edge lengths, mm		
Superior	Lower edge of CN V	10.13 ± 2.45
Posterior	QBL	9.03 ± 1.75
Inferior	SVN	11.5 ± 2.43
Anterior	Petrous Bone	12.6 ± 0.76
Area of ITT, mm²		
ITT Vertex Angles, °		
Anterosuperior vertex	Petrous Bone - CN V	67.41 ± 14.57
Posterosuperior vertex	QBL - CN V	126.52 ± 15.82
Posteroinferior vertex	QBL - SVN	77.21 ± 9.41
Anteroinferior vertex	Petrous Bone - SVN	88.86 ± 11.4

Table 2: Measurements of ITT

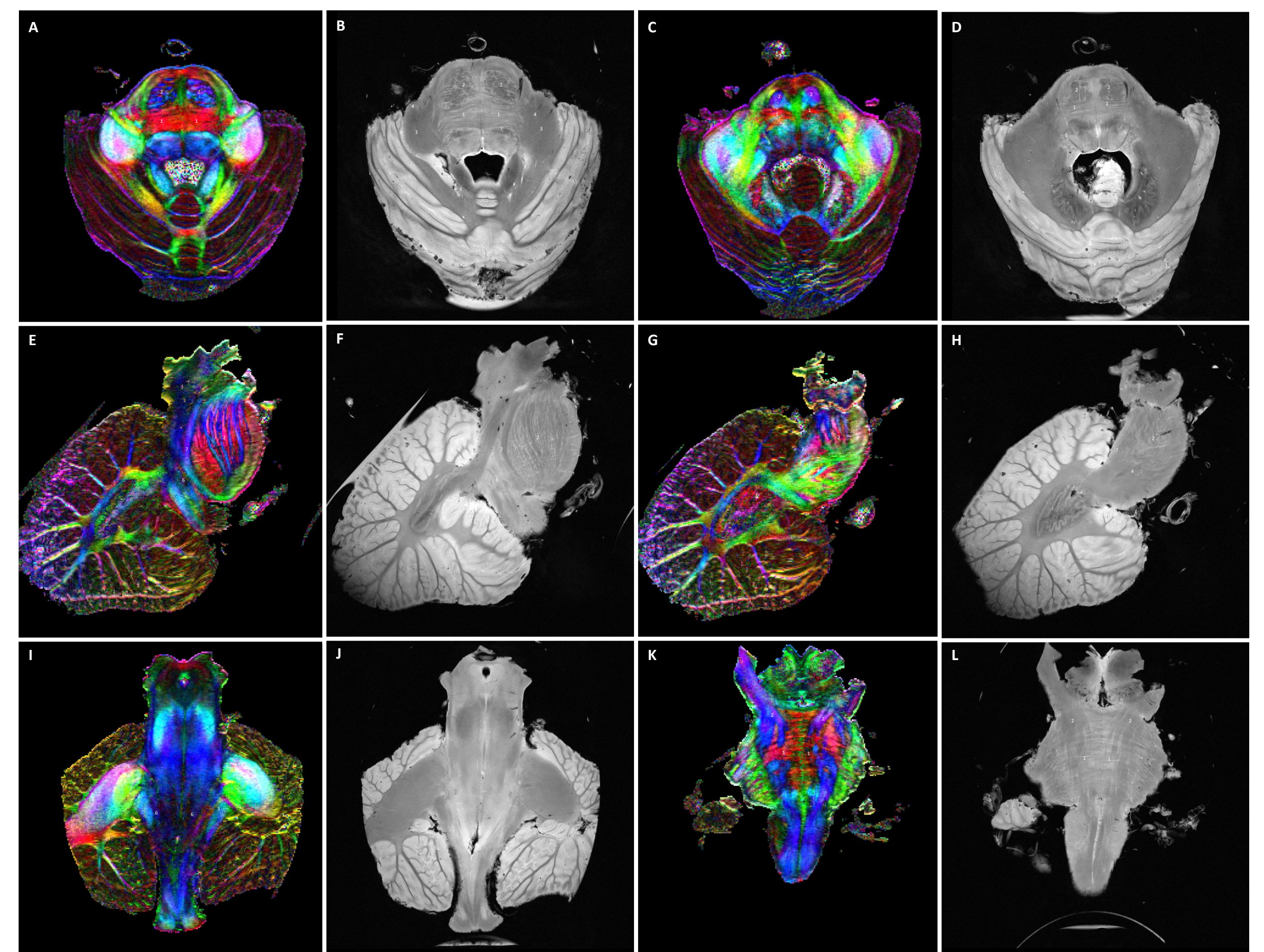


Figure 4: Ultra-high-resolution 7-T magnetic resonance imaging (MRI) and corresponding fractional anisotropy (FA) color maps illustrate the fiber tracts and key anatomical structures related to the STT and ITT.

(1) lateral pontine fibers, (2) corticospinal tract, (3) inferior cerebellar peduncle, (4) fiber tracts of the cranial nerve V inside the brainstem, (5) fiber tracts of the cranial nerve VII inside the brainstem, (6) facial nucleus, (7) medial lemniscus

Conclusions

STT and ITT represent consistent and surgically expandable microsurgical landmarks for accessing the upper cerebellopontine cistern. Quantitative assessment highlights their relevance in operative planning for peritrigeminal cavernous malformations. Together, these triangles create the largest available corridors to the anterolateral pons and provide direct access to adjacent safe entry zones, making them particularly valuable in the treatment of peritrigeminal pontine cavernous malformations and complex basilar-peritrigeminal lesions.

Contact

Kivanc Yangi, M.D.
Dept. of Neurosurgery, Barrow Neurological Institute
St. Joseph's Hospital and Medical Center
2910 N 3rd Ave, 85013, Phoenix, Arizona, USA
kivancyangi@gmail.com
602-767-9802

References

- Benner D, Hendricks BK, Benet A, et al. A system of anatomical triangles defining dissection routes to brainstem cavernous malformations: definitions and application to a cohort of 183 patients. *J Neurosurg.* 2022;138(3):768-784. Published 2022 Aug 26. doi:10.3171/2022.6.JNS212907
- Catapano JS, Rumalla K, Srinivasan VM, Lawrence PM, Larson Keil K, Lawton MT. A taxonomy for brainstem cavernous malformations: subtypes of pontine lesions. Part 1: basilar, peritrigeminal, and middle peduncular. *J Neurosurg.* 2022;137(5):1462-1476. Published 2022 Mar 25. doi:10.3171/2022.1.JNS212690